



# Photobiomodulation can alter mRNA levels cell death-related

Pierre Augusto Victor da Silva<sup>1</sup> · Lúcia Mara Januário Dos Anjos<sup>2</sup> · Thais Fraga Abduch<sup>3</sup> · Rafael Pereira<sup>4</sup> · Adenilson de Souza da Fonseca<sup>5</sup> · Fátia de Paoli<sup>2</sup>

Received: 18 November 2018 / Accepted: 21 January 2019 / Published online: 5 February 2019  
© Springer-Verlag London Ltd., part of Springer Nature 2019

## Abstract

Photobiomodulation (PBM) by low-level laser has demonstrated excellent results for inflammatory treatments, promoting repair of injured tissues. Knowledge regarding the molecular mechanisms involved in this process has been increasing, but its effect on cell death/survival-related gene expression after laser irradiation with different doses is not well understood. So, it is important to know these effects in order to guarantee the safety of therapeutic protocols based on PBM. This study aimed to investigate the mRNA levels of genes related to proteins involved in cell death/survival pathways of healthy tissues from talocrural joint of mice after PBM. Mice were divided into three groups: control, PBM at 3 J cm<sup>-2</sup>, and PBM at 30 J cm<sup>-2</sup>. Laser irradiation was performed on talocrural joint during four consecutive days. Morphological analyses, immunocytochemistry, FasL, Fas, Bax, Apaf1, Caspase9, Caspase3, Caspase6, Bcl2 mRNA levels, and DNA fragmentation were performed to verify cell death induction after laser irradiation. PBM can increase mRNA levels of almost genes pro-apoptotic. On the other hand, mRNA level of anti-apoptotic protein Bcl-2 gene was not significantly altered. Bcl-2/Bax ratio (indicator of protective molecular response) was decreased after PBM at 30 J cm<sup>-2</sup>, trending to DNA fragmentation. Results obtained in this study indicate that PBM by low-level infrared laser alters mRNA relative levels of genes involved in cell death pathways. However, these molecular alterations were not able to cause DNA fragmentation in cells in talocrural joint tissues, indicating that infrared laser was not enough to cause cell death.

**Keywords** Photobiomodulation · Apoptosis · Bcl-2/Bax ratio · Caspase · DNA fragmentation

✉ Pierre Augusto Victor da Silva  
pierreaugusto@gmail.com

- <sup>1</sup> Departamento de Fisioterapia, Centro Universitário Redentor (UniRedentor), BR 356, nº 25 - Cidade Nova, Itaperuna / Rio de Janeiro 28300-000, Brazil
- <sup>2</sup> Departamento de Morfologia, Instituto de Ciências Biológicas, Universidade Federal de Juiz de Fora, Rua José Lourenço Kelmer, s/n-Campus Universitário, São Pedro, Juiz de Fora, Minas Gerais 36036-900, Brazil
- <sup>3</sup> Departamento de Fisioterapia, Faculdade de Ciências Médicas e da Saúde (SUPREMA), Alameda Salvaterra, nº. 200, Bairro Salvaterra, Juiz de Fora, Minas Gerais 36033-003, Brazil
- <sup>4</sup> Departamento de Ciências Biológicas, Universidade Estadual do Sudoeste da Bahia (UESB), Jequié, Bahia 45210-506, Brazil
- <sup>5</sup> Departamento de Biofísica e Biometria, Instituto de Biologia Roberto Alcântara Gomes, Universidade do Estado do Rio de Janeiro, Avenida 28 de Setembro, 87, Vila Isabel, Rio de Janeiro 20551-030, Brazil

## Abbreviations

µm	Micrometers
AlGaAs	Gallium arsenide aluminum
AMPC	Adenosine monophosphate cyclic
APAF-1	“Apoptotic protease-activating factor 1” or apoptosis factor 1 activating protease
ATP	Adenosine triphosphate
BAK	Member of the pro-apoptotic Bcl-2 family
BAX	Member of the pro-apoptotic Bcl-2 family
Bcl-2	B cell lymphoma protein 2
BH3	Member of the pro-apoptotic Bcl-2 family
BID	Member of the pro-apoptotic Bcl-2 family
BAD	Member of the pro-apoptotic Bcl-2 family
Caspase	Cysteine-specific protease aspartyl
cDNA	Complementary deoxyribonucleic acid
DISC	Death-inducing signaling complex
DNA	Deoxyribonucleic acid
EROs	Reactive oxygen species
FADD	“Fas-associated death domain” or FAS-associated death domain

FAS or CD95 or APO-1	Pro-apoptosis membrane receptor or protein
F A S - L o r CD95L	FAS-binding membrane protein
IL-1	Interleukin 1
IL-17	Interleukin 17
J/cm <sup>2</sup>	Joules per square centimeters
LASER	Light amplification by stimulated emission of radiation
mJ	Millijoules
MMP	Matrix metalloproteinases
mW	Milliwatt
nm	Nanometers
PBS	Saline phosphate-buffered solution
PCR	Polymerase chain reaction
RNA	Ribonucleic acid
RNS	Reactive nitrogen species
t-BID	Truncated BID
TdT	Terminal deoxynucleotidyl transferase
TGF- $\beta$	Transforming growth factor $\beta$
TNF	Tumor necrosis factor
TNFR1	TNF receptor
TUNEL POD	Peroxidase-labeled antibody used for the detection of apoptosis (programmed cell death) with the TUNEL reaction followed by microscopy

## Introduction

Photobiomodulation (PBM) effect induced by low-level lasers has been widely used in many rehabilitation programs with promising results [1, 2] for treatment of orthopedic and rheumatic disorders, such as muscle and tendon injuries [3], rheumatoid diseases (rheumatoid arthritis and osteoarthritis) [4], fibromyalgia [5], low back pain [6–8], and carpal tunnel syndrome [9]. Several molecular mechanisms were proposed to explain the benefits of laser irradiation and the most accepted for cell-light interaction was proposed by Karu [10], referring to retrograde mitochondrial signaling, which occurs by light activation at visible and infrared region of electromagnetic spectrum. It is reported that alterations on mitochondrial membrane potential and permeability lead to ATP synthesis increase, change the calcium ion homeostasis, and increase of reactive oxygen species (ROS) production [10]. Some of these immediate events (i.e., occurred along some minutes after laser irradiation) lead to cascade of cellular signaling and molecular responses [11], culminating in changes on gene expressions [11–14].

When an area is irradiated, cells absorb energy from monochromatic (laser) radiation [11, 15], inducing cell responses. All tissues irradiated in this area (healthy or not)

may respond it differently, since laser irradiation is not habitual for them. According to Hamblin [15, 16], cells present biphasic-dose response to PBM, in which stimulatory or inhibitory effects can be observed. The type of cell response would be conditioned to time exposure and doses. Thus, the challenge for researches involving PBM is to establish safe doses for rehabilitation treatments, focusing injured tissues and to understand that irradiated area involves not only injured but also healthy tissues. Thereby, these findings may also help to understand molecular mechanisms related to beneficial and adverse laser-induced effects.

Previous studies of inflammatory models demonstrated that apoptosis occurs mainly in inflammatory cells while this process does not occur in other cells (healthy cells close to inflammatory area) [17, 18]. This indicates that different cell types may express different mechanisms of death/survival at different thresholds. It was described that inflammatory cells have additional mechanisms for free radical production [15, 19], and this may explain selective effects of PBM. Also, some authors have reported induction of apoptotic process in healthy tissues after PBM [20–22].

Apoptosis is initiated by formation of multiprotein complexes, including death signaling complex. This complex is generated after binding of extracellular death ligands to death receptors (extrinsic pathway) and/or by cytochrome c release from mitochondria (intrinsic pathway). Both pathways recruit and activate caspases, including effector caspases, targeting specific cellular and nuclear substrates for proteolysis. After signaling apoptosis, modifications occur within cell, including caspase activation that cleaves cellular components necessary for normal functions, such as cytoskeletal and nuclear proteins. Cytoskeleton reorganization and DNA fragmentation by endonucleases are promoted by effector caspases (caspase 3, for example), culminating in apoptotic body formation [23–25].

The mitochondrial pathway is regulated by both anti-apoptotic Bcl-2 family proteins (Bcl-2, Bcl-x, Bcl-XL, Bcl-XS, Bcl-w, and BAG) and pro-apoptotic proteins (Bax, Bak, Bid, Bad, Bim, Bik, and Blk). Pro-apoptotic proteins stimulate cytochrome c release from mitochondria that, together with Apaf-1, form a complex called apoptosome [25–27]. On the other hand, anti-apoptotic Bcl-2 family prevents apoptogenic factors release from mitochondria, including cytochrome c [28]. So, cellular resistance to apoptotic stimuli is due to balance between anti-apoptotic and pro-apoptotic proteins [29].

Since different cell types have mechanisms of death/survival at different thresholds and molecular mechanisms involved in PBM are not understood yet, this study aimed to investigate mRNA levels of genes related to cell death pathways in tissues from talocrural joint after PBM by low-level infrared laser irradiation.

## Material and methods

Experiments were approved by Ethics Committee of Federal University of Juiz de Fora (protocol 039/2014) and conducted in accordance with international ethical standards.

### Animals

Eighteen male C57BL/6 mice aged 8–10 weeks, body weight between 24 and 28 g, were kept in a controlled environment (temperature  $25^{\circ} \pm 2^{\circ}\text{C}$ , light/dark cycle of 12/12 h). Animals were randomly distributed into three groups ( $n = 6$ ): (i) control—not irradiated with low-level laser, (ii)  $3\text{ J cm}^{-2}$ —irradiated with low-level laser at  $3\text{ J cm}^{-2}$ , and (iii)  $30\text{ J cm}^{-2}$ —irradiated with low-level laser at  $30\text{ J cm}^{-2}$ .

### Low-level laser

A low-level infrared laser (AlGaAs laser; HTM Indústria de Equipamentos Eletro-eletrônicos Ltda, Brazil) was used in this study. The laser parameters were wavelength 830 nm, power output of 10 mW, laser beam area of  $0.05\text{ cm}^2$ , power density of  $0.2\text{ W cm}^{-2}$ , and energy densities of 3 and  $30\text{ J cm}^{-2}$  (a total energy of 150 and 1500 mJ after 15 and 150 s, respectively) in continuous wave emission mode.

Animals were immobilized and laser irradiations were performed for 4 consecutive days on both talocrural joints. Twenty-four hours after the last laser irradiation, the animals were anesthetized with ketamine hydrochloride ( $80\text{ mg kg}^{-1}$ ; Syntec, Brazil) and xylazine hydrochloride ( $20\text{ mg kg}^{-1}$ ; Syntec, Brazil) intraperitoneally and then cervical dislocation was performed, as approved by local Animal Experimentation Committee. Joints were dissected, skin removed, washed in distilled water to remove blood, and distributed to morphological and immunohistochemical analysis (right joints) and real-time PCR analysis (left joints).

### Total RNA extraction and real-time PCR

After skin and muscle removal, the left joints were immersed in liquid nitrogen, macerated, and total RNA was extracted by phenolic buffer technique. Briefly, TRIzol® reagent (Invitrogen, USA) was added and centrifuged (12,000 rpm,  $4^{\circ}\text{C}$ , 10 min). The supernatants were transferred to other tubes, chloroform was added, mixtures were centrifuged (12,000 rpm,  $4^{\circ}\text{C}$ , 15 min), aqueous phases were transferred to other tubes, and isopropanol was added. After incubation at room temperature for 15 min the mixtures were centrifuged (12,000 rpm,  $4^{\circ}\text{C}$ , 10 min), supernatants were discarded, and precipitate was washed with ethanol-DEPC solution (80% ethanol, 0.1%) and centrifuged. Supernatants were removed and total RNA was reconstituted in water-DEPC solution (0.1%). The concentration and purity of RNA was determined

by spectrophotometer, calculating optical density ratio at wavelength ratio of 260/280 nm. Then, 2  $\mu\text{g}$  of total RNA was transcribed into complementary DNA (cDNA) using cDNA Reverse Transcription Kit (Applied Biosystems, USA) following manufacturer's guidelines. Primers for quantitative real-time polymerase chain reaction (RT-qPCR) were designed using Primer 3 program [17, 30], on different exons in order to avoid the possibility of contamination with genomic DNA. Real-time PCR assay was performed using Step One Plus™ Real Time PCR System instrument (Applied Biosystems, USA) under following conditions: 40 cycles; on each cycle, initial denaturation at  $95^{\circ}\text{C}$  for 10 min, denaturation at  $95^{\circ}\text{C}$  for 15 s, and primer pairing and extension at  $60^{\circ}\text{C}$  for 1 min. For analysis of gene expression,  $2^{-\Delta\Delta\text{CT}}$  method was used [31]. As an internal control,  $\beta$ -actin was used.

### Histological procedures

Right joints were dissected and fixed in 4% paraformaldehyde solution for 24 h, decalcified in 5% nitric acid for 48 h, dehydrated, and embedded in histosec® paraffin (Merck, Germany). Sagittal sections (4  $\mu\text{m}$  thick) were used for TUNEL analysis.

### DNA fragmentation

DNA fragmentation was detected using a TUNEL POD assay (Roche, Germany) according to manufacturer's manual. After deparaffinization and permeabilization, tissue sections were incubated in proteinase K for 15 min at room temperature. Sections were then incubated in TUNEL reaction mixture containing terminal deoxynucleotidyl transferase (TdT) and fluorescein-dUTP at  $37^{\circ}\text{C}$  for 1 h. After washing three times with phosphate-buffered solution (PBS), sections were incubated with Converter-POD containing horseradish peroxidase-conjugated anti-fluorescein antibody (POD) at room temperature for 30 min. After washing three times with PBS, these sections were incubated with 3-3'-diaminobenzidine (Sigma-Aldrich, USA) for 10 min at room temperature ( $25^{\circ}\text{C}$ ) and then stained with methyl green [17].

### Image analyses

Morphological and quantitative analyses were performed using Olympus microscope (BX53F), equipped with U-PlanFL N 4/0.13, 10/0.30, 40/0.75, and 100/0.85 objectives. Images were captured by Olympus DP73 camera, using cell Sens Image software (version 5.1, Olympus, USA). For quantitative analysis, objective 40/0.75 was used. Image Pro Plus software (Media Cybernetics, Inc.) was used for quantification of positive TUNEL POD cell labeling.

## Statistical analysis

Normality of data was tested by Shapiro-Wilk test. Considering that most variables did not exhibit a normal distribution, results were presented as median  $\pm$  interquartile range. For variables with normal distribution, analysis of variance (ANOVA) was used for group comparisons followed by appropriate post hoc tests with Bonferroni corrections when significant differences were identified. For other variables, Kruskal-Wallis test was used for group comparisons followed by Dunn's test as post hoc test when significant differences were identified. Significance level for all tests was set as  $p \leq 0.05$ . GraphPad software (GraphPad Prism VII Software, San Diego, CA, USA) was used for all statistical analysis and graphical design.

## Results

### Relative gene expressions related to apoptosis

Figure 1a, b shows that relative mRNA levels of genes related to apoptotic pathways were altered after infrared laser exposure at 3 and 30 J cm<sup>-2</sup>, when compared with control group. Results indicate that infrared laser irradiation at both energy densities increased Bax and Fas mRNA levels, while FasL, Caspase 9, Caspase 3, and Caspase 6 mRNA levels were increased only at 3 J cm<sup>-2</sup>. Also, Apaf1 mRNA level was increased only at 30 J cm<sup>-2</sup> when compared with control group.

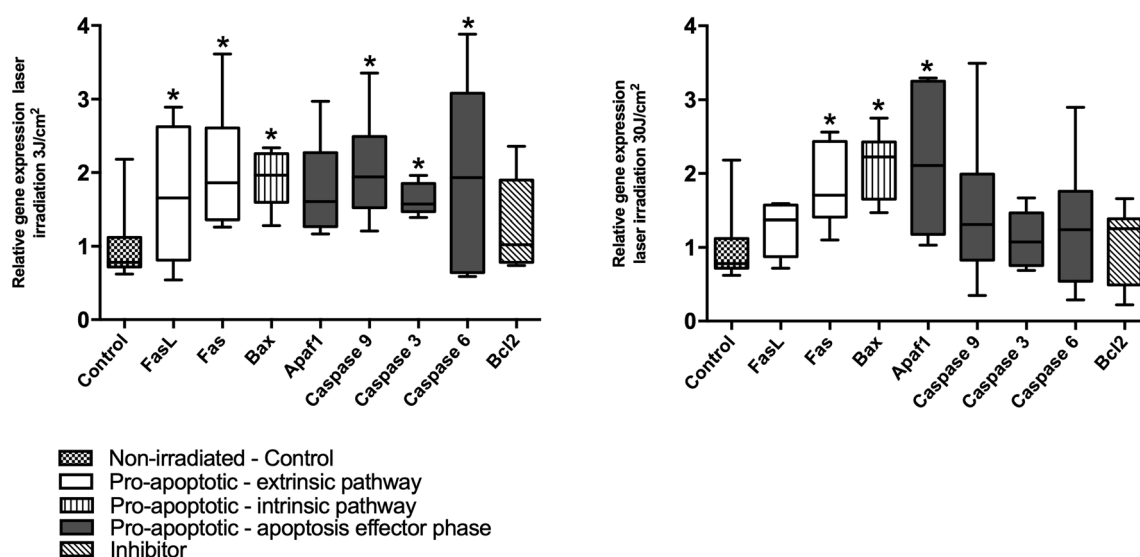


**Fig. 1** Median  $\pm$  interquartile range of mRNA levels for genes related to apoptotic pathways after laser irradiation at 3 J cm<sup>-2</sup> (a) and 30 J cm<sup>-2</sup> (b). \*Significantly different ( $p < 0.05$ )

## Ratio Bcl-2/Bax

The Bcl-2/Bax ratio was used as indicator of apoptotic potential, such as high ratios indicate anti-apoptosis profile and low ratios indicate apoptosis profile. Bcl-2/Bax ratio for animals from 30-J cm<sup>-2</sup> group was decreased when compared with control group. This result was not observed for group laser irradiated at 3 J cm<sup>-2</sup> (Fig. 2).

## Morphological analysis and DNA fragmentation

Morphological changes were not observed after infrared laser irradiation for both energy densities evaluated. All tissues present in talocrural joint (articular cartilage, connective tissue, and bone) did not present morphological characteristic altered after infrared laser irradiation.

DNA fragmentation was detected only in cells from connective tissues, while cells from articular cartilage and bone did not present positive labeling. However, quantitative analysis indicated no statistical differences ( $p > 0.05$ ) after infrared laser irradiation for both energy densities evaluated (Fig. 3).

## Discussion

Although PBM has been widely used in various therapeutic forms for treatment of disorders [1, 2, 18, 32–35], experimental investigations are necessary for a better understanding of cell responses, becoming this therapy safer and more effective. Most of these studies describe good results for PBM but there are also in literature studies suggesting sub-lethal DNA damages and apoptosis induction [22, 36]. As cells show

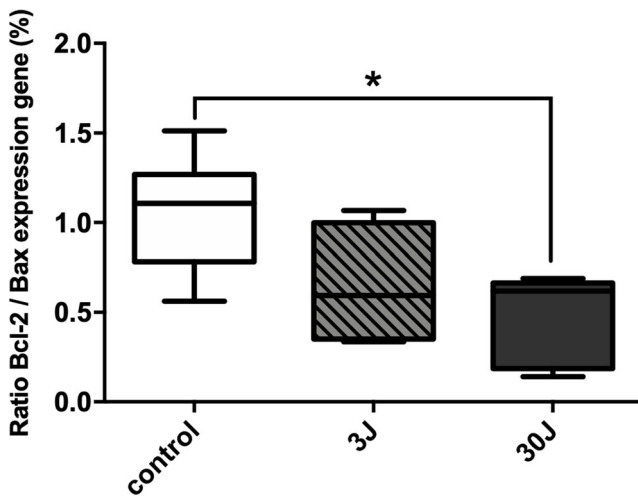


**Fig. 2** Median  $\pm$  interquartile range of the Bcl-2/Bax mRNA level ratio of control and laser irradiated groups at 3 and 30 J cm<sup>-2</sup>. \*Significantly different ( $p < 0.05$ )

biphasic dose response (stimulatory or inhibitory effects) to PBM [15, 16], the type of cellular response would be conditioned by time irradiation and laser doses [33, 37]. Following that, we investigated whether apoptosis mechanisms would be active in different cells from tissues present in talocrural joint

after PBM by low-level infrared laser, comparing two different energy densities (3 and 30 J cm<sup>-2</sup>).

Since light is absorbed by mitochondria and it plays a key role in apoptotic processes, cell death could be triggered through extrinsic and intrinsic pathways. mRNA levels for genes involved in both pathways were altered at two energy densities evaluated (3 and 30 J cm<sup>-2</sup>). Extrinsic pathway-mediated apoptosis is activated when certain ligands, such as Fas-L, bind at death receptors on plasma membrane, leading to cytoplasmatic signaling and caspase-8 activation [38, 39]. Formation of active caspase-8 will act as caspase initiator, which in turn acts other effector caspases (such as caspase-3 and -6) [39–42]. Our results show that Fas, Fas-L, caspases-3, -6, and -9 mRNA levels were upregulated after laser irradiation at 3 J cm<sup>-2</sup>. On the other hand, only Fas mRNA level was increased after laser irradiation at 30 J cm<sup>-2</sup> when compared with control group. Intrinsic pathway is directly related to mitochondria, especially via Bid and Bax proteins (two pro-apoptotic proteins present in Bcl-2 family). These proteins promote cytochrome c release from mitochondrial intermembrane space to cytoplasm. Once in cytoplasm, cytochrome c binds to adaptor protein Apaf-1, which is able to activate caspase-9 and, possibly, other initiator caspases. Bax mRNA level was altered after laser irradiation for both energy

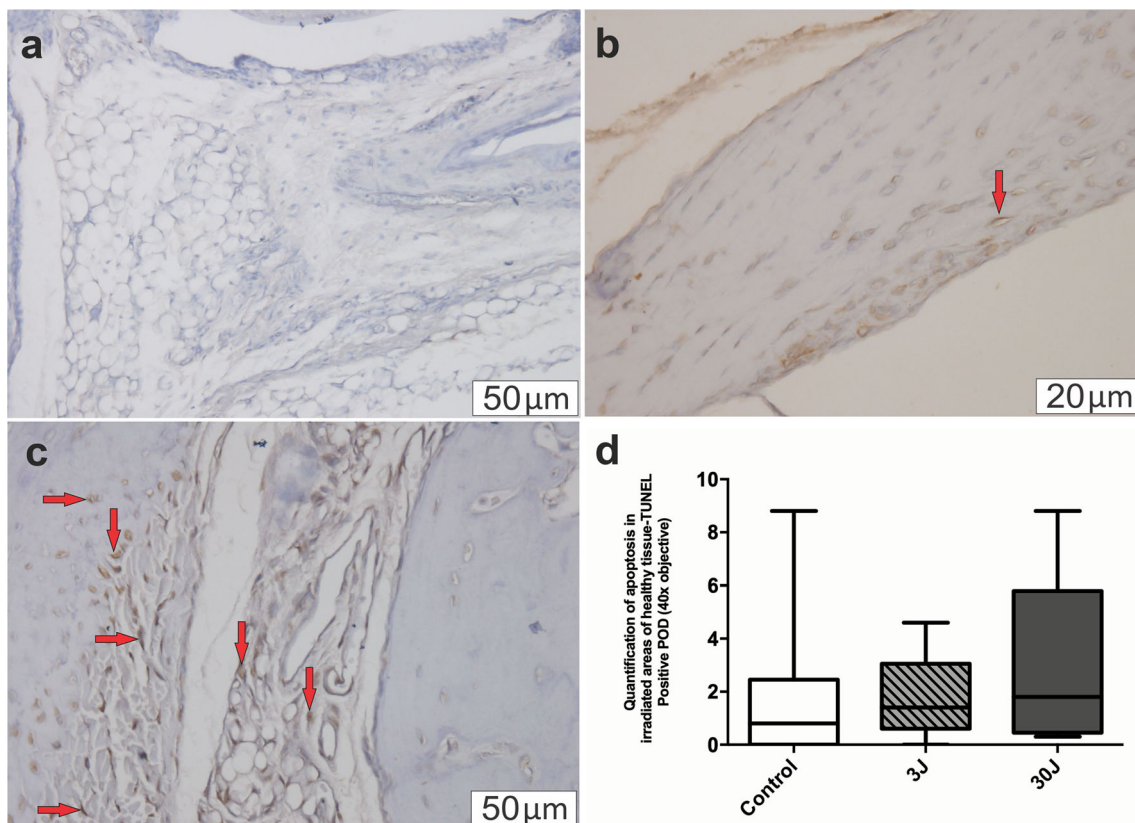


**Fig. 3** Representative images demonstrate DNA fragmentation in tissues from mouse talocrural joint. **a** Control. **b** 3 J cm<sup>-2</sup>. **c** 30 J cm<sup>-2</sup>. **d** Quantification of positive cell labeling (median  $\pm$  interquartile). There were no significant differences. Arrow indicates positive cell labeling

densities tested, while Apaf1 mRNA relative level was increased only after laser irradiation at  $30 \text{ J cm}^{-2}$  (Fig. 1a, b).

Bcl-2 family presents a range of bioactivities from inhibition up to promotion of apoptosis [43]. While Bax and Bid proteins can release cytochrome c from mitochondrial intermembrane space to cytoplasm, Bcl-2 protein prevents cytochrome c release, acting as a regulator or inhibitor of apoptosis. Also, this protein contributes to inhibition of ROS generation and intracellular acidification, thereby stabilizing the membrane potential of mitochondria [44, 45]. Bax can act by binding to Bcl-2, promoting formation of apoptosome (complex formed by APAF-1 and activated caspase-9) leading to apoptosis. Moreover, Bax can also promote apoptosis through interaction with mitochondria, independently of interaction with anti-apoptotic proteins [46]. Bcl-2/Bax ratio, when equilibrated, acts as regulatory effect in apoptosis [28]. In our results, Bax mRNA level was increased but Bcl-2 mRNA level was not altered after  $30 \text{ J cm}^{-2}$ , which may be indicative of stimulus to cell death.

Morphologically, apoptosis is characterized by chromatin condensation and DNA fragmentation, followed by nuclear membrane disruption and apoptotic body formation [22, 47]. This fragmentation is consequence of cascade caspases that, when activated, moves towards to nucleus causing DNA fragmentation. Although TUNEL result did not demonstrate statistical differences after laser irradiation for both energy densities tested, it demonstrated a tendency of fragmentation after laser irradiation at higher energy density ( $30 \text{ J cm}^{-2}$ ). In this group, positive cell labeling was well observed in cells from connective tissue present in synovial membranes. In addition, no positive cell labeling was observed in bone and articular cartilage cells. In previous study, DNA fragmentation and loss of chromatin in tendons (connective tissue) is reported as a consequence of PBM by low-level infrared laser (same equipment, but different energy densities); both events are related to apoptosis process [22]. In addition, these different cell responses could indicate more sensibility to light absorption of fibroblasts than other cells. These are important findings for joint injury rehabilitation using PBM, since local tissues could respond in different ways. So, it is important to point out that irradiated area involves not only inflammatory cells but also healthy tissues and PBM may cause apoptosis stimuli in cells not injured.

Although the mRNA levels for almost pro-apoptotic genes were increased and anti-apoptotic mRNA levels were not altered, cell death was not completely implemented. PBM was able to alter mRNA levels for pro-apoptotic genes, both involved in extrinsic and intrinsic pathways, but somehow this stimulus is not enough to drive cells to death. However, it has been previously described that PBM at high energy densities induces apoptosis by activation of caspase-3 and alteration of mitochondrial permeability [33].

Therefore, our research suggests that good clinical practice responses to PBM depend not only on physical laser irradiation parameters but also on understanding of tissues involved and their different responses for laser parameters. This study could contribute to safer therapies decreasing possible side effects from PBM when used for treatment of joint injury.

## Conclusion

The results obtained in this study indicate that PBM can alter mRNA levels of genes involved in cell death pathways. However, these molecular alterations were not able to cause DNA fragmentation in cells from talocrural joint tissues, indicating that this stimulus is not enough to drive cell to death.

**Funding** This study was supported by Conselho Nacional de Pesquisa e Desenvolvimento-CNPq (process number APQ 474405/2013–3) and Fundação de Amparo à Pesquisa do Estado de Minas Gerais-FAPEMIG (process number APQ 02123/15).

## Compliance with ethical standards

**Conflict of interest** The authors declare that they have no conflict of interests.

**Publisher's note** Springer Nature remains neutral with regard to jurisdictional claims in published maps and institutional affiliations.

## References

1. Leal-Junior ECP, Vanin AA, Miranda EF et al (2015) Effect of phototherapy (low-level laser therapy and light-emitting diode therapy) on exercise performance and markers of exercise recovery: a systematic review with meta-analysis. *Lasers Med Sci* 30:925–939. <https://doi.org/10.1007/s10103-013-1465-4>
2. Borges LS, Cerqueira MS, Dos Santos Rocha JA et al (2013) Light-emitting diode phototherapy improves muscle recovery after a damaging exercise. *Lasers Med Sci* 29:1139–1144. <https://doi.org/10.1007/s10103-013-1486-z>
3. David R, De Souza RA, Xavier M et al (2010) Anti-inflammatory effects of low-level light emitting diode therapy on Achilles tendinitis in rats 558:553–558. <https://doi.org/10.1002/lsm.20896>
4. Baltzer AWA, Stosch D, Seidel F, Ostapczuk MS (2017) Low level laser therapy : A narrative literature review on the efficacy in the treatment of rheumatic orthopaedic conditions. *Z Rheumatol* 76(9): 806–812
5. Ruaro JA, Fréz AR, Ruaro MB, Nicolau RA (2014) Low-level laser therapy to treat fibromyalgia. *Lasers Med Sci* 29(6):1815–1819
6. Kingsley JD, Demachak T, Mathis R (2014) Low-level laser therapy as a treatment for chronic pain. *Front Physiol* 5:1–3. <https://doi.org/10.3389/fphys.2014.00306>
7. Djavid GE, Mehrdad R, Ghasemi M et al (2007) In chronic low back pain, low level laser therapy combined with exercise is more beneficial than exercise alone in the long term: a randomised trial.

- Aust J Physiother 53:155–160. [https://doi.org/10.1016/S0004-9514\(07\)70022-3](https://doi.org/10.1016/S0004-9514(07)70022-3)
8. Glazov G, Yelland M, Emery J (2016) Low-level laser therapy for chronic non-specific low back pain: a meta-analysis of randomised controlled trials. *Acupunct Med* 34:328–341. <https://doi.org/10.1136/acupmed-2015-011036>
  9. Li Z-J, Wang Y, Zhang H-F et al (2016) Effectiveness of low-level laser on carpal tunnel syndrome: a meta-analysis of previously reported randomized trials. *Medicine (Baltimore)* 95:e4424. <https://doi.org/10.1097/MD.0000000000004424>
  10. Karu TI (2008) Mitochondrial signaling in mammalian cells activated by red and near-IR radiation. *Photochem Photobiol* 84:1091–1099. <https://doi.org/10.1111/j.1751-1097.2008.00394.x>
  11. Karu T (2014) Cellular and Molecular Mechanisms of Photobiomodulation (Low-Power Laser Therapy). *IEEE J Sel Top Quantum Electron* 20(2):143–148
  12. Wu S, Xing D (2014) Intracellular signaling cascades following light irradiation. *Laser Photon Rev* 8:115–130. <https://doi.org/10.1002/lpor.201300015>
  13. Song S, Zhang Y, Fong C-C et al (2003) cDNA microarray analysis of gene expression profiles in human fibroblast cells irradiated with red light. *J Invest Dermatol* 120:849–857. <https://doi.org/10.1046/j.1523-1747.2003.12133.x>
  14. Calles C, Schneider M, MacAluso F et al (2010) Infrared a radiation influences the skin fibroblast transcriptome: mechanisms and consequences. *J Invest Dermatol* 130:1524–1536. <https://doi.org/10.1038/jid.2010.9>
  15. Huang Y-Y, Chen AC-H, Carroll JD, Hamblin MR (2009) Biphasic dose response in low level light therapy. Dose-Response 7:dose-response.0. <https://doi.org/10.2203/dose-response.09-027.Hamblin>
  16. Huang Y-Y, Sharma SK, Carroll J, Hamblin MR (2011) Biphasic dose response in low level light therapy – an update. Dose-Response 9:dose-response.1. <https://doi.org/10.2203/dose-response.11-009.Hamblin>
  17. dos Anjos LMJ, da Fonseca A d S, Gameiro J, de Paoli F (2017) Apoptosis induced by low-level laser in polymorphonuclear cells of acute joint inflammation: comparative analysis of two energy densities *Lasers Med Sci* 32:975–983. <https://doi.org/10.1007/s10103-017-2196-8>
  18. Sergio LPS, Campos VMA, Vicentini SC et al (2016) Low-intensity red and infrared lasers affect mRNA expression of DNA nucleotide excision repair in skin and muscle tissue. *Lasers Med Sci* 31:429–435. <https://doi.org/10.1007/s10103-016-1870-6>
  19. Sergio LPDS, Thomé AMC, Trajano LADSN et al (2018) Photobiomodulation prevents DNA fragmentation of alveolar epithelial cells and alters the mRNA levels of caspase 3 and Bcl-2 genes in acute lung injury. *Photochem Photobiol Sci* 17:975–983. <https://doi.org/10.1039/c8pp00109j>
  20. Huang L, Wu S, Xing D (2011) High fluence low-power laser irradiation induces apoptosis via inactivation of Akt/GSK3 $\beta$  signaling pathway. *J Cell Physiol* 226:588–601. <https://doi.org/10.1002/jcp.22367>
  21. Wu S, Xing D, Gao X, Chen WR (2009) High fluence low-power laser irradiation induces mitochondrial permeability transition mediated by reactive oxygen species. *J Cell Physiol* 218:603–611. <https://doi.org/10.1002/jcp.21636>
  22. De Paoli F, Ramos Cerqueira L, Martins Ramos M et al (2014) DNA fragmentation and nuclear phenotype in tendons exposed to low-intensity infrared laser. *Prog Biomed Opt Imaging - Proc SPIE* 9321:1–12. <https://doi.org/10.1117/12.2075726>
  23. Hassan M, Watari H, Abualmaaty A, et al (2014) Apoptosis and molecular targeting therapy in cancer. *Biomed Res Int* 2014:150845
  24. Zaman S, Wang R, Gandhi V (2014) Targeting the apoptosis pathway in hematologic malignancies. *Leuk Lymphoma* 55:1980–1992. <https://doi.org/10.3109/10428194.2013.855307>
  25. Pfeiffer CM, Singh ATK (2018) Apoptosis: a target for anticancer therapy. *Int J Mol Sci* 19:448. <https://doi.org/10.3390/jms19020448>
  26. Nagata S (2018) Apoptosis and Clearance of Apoptotic Cells. *Annu Rev Immunol* 36(1):489–517. <https://doi.org/10.1146/annurev-immunol-042617-053010>
  27. Yuan S, Akey CW (2013) Apoptosome structure, assembly, and procaspase activation. *Structure* 21:501–515. <https://doi.org/10.1016/j.str.2013.02.024>
  28. Bialik S, Zalckvar E, Ber Y et al (2010) Systems biology analysis of programmed cell death. *Trends Biochem Sci* 35:556–564. <https://doi.org/10.1016/j.tibs.2010.04.008>
  29. Ashkenazi A (2008) Targeting the extrinsic apoptosis pathway in cancer. *Cytokine Growth Factor Rev* 19:325–331. <https://doi.org/10.1016/j.cytogfr.2008.04.001>
  30. Untergasser A, Cutcutache I, Koressaar T et al (2012) Primer3 — new capabilities and interfaces. *Nucleic Acids Res* 40:1–12. <https://doi.org/10.1093/nar/gks596>
  31. Livak KJ, Schmittgen TD (2001) Analysis of relative gene expression data using real-time quantitative PCR and the 2- $\Delta\Delta$ CT method. *Methods* 25:402–408. <https://doi.org/10.1006/meth.2001.1262>
  32. Carroll JD, Milward MR, Cooper PR et al (2014) Developments in low level light therapy (LLLT) for dentistry. *Dent Mater* 30:465–475. <https://doi.org/10.1016/j.dental.2014.02.006>
  33. de Freitas LF, Hamblin MR (2016) Proposed mechanisms of Photobiomodulation or low-level light therapy. *IEEE J Sel Top Quantum Electron* 22(3). <https://doi.org/10.1109/JSTQE.2016.2561201>
  34. De Marchi T, Leal ECP, Bortoli C et al (2012) Low-level laser therapy (LLLT) in human progressive-intensity running: effects on exercise performance, skeletal muscle status, and oxidative stress. *Lasers Med Sci* 27:231–236. <https://doi.org/10.1007/s10103-011-0955-5>
  35. Dos Santos Maciel T, Muñoz ISS, Nicolau RA et al (2014) Phototherapy effect on the muscular activity of regular physical activity practitioners. *Lasers Med Sci* 29:1145–1152. <https://doi.org/10.1007/s10103-013-1481-4>
  36. Canuto KS, Sergio LPS, Guimarães OR et al (2015) Low-level red laser therapy alters effects of ultraviolet C radiation on *Escherichia coli* cells. *Braz J Med Biol Res* 48(10):939–944
  37. Sun X, Wu S, Xing D (2010) The reactive oxygen species-Src-Stat3 pathway provokes negative feedback inhibition of apoptosis induced by high-fluence low-power laser irradiation. *FEBS J* 277:4789–4802. <https://doi.org/10.1111/j.1742-4658.2010.07884.x>
  38. Czabotar PE, Lessene G, Strasser A, Adams JM (2014) Control of apoptosis by the BCL-2 protein family: implications for physiology and therapy. *Nat Rev Mol Cell Biol* 15:49–63. <https://doi.org/10.1038/nrm3722>
  39. Strasser A, Jost PJ, Nagata S (2009) Review the many roles of FAS receptor signaling in the immune system. *Immunity* 30:180–192. <https://doi.org/10.1016/j.immuni.2009.01.001>
  40. Jost PJ, Grabow S, Gray D et al (2009) LETTERS XIAP discriminates between type I and type II. *Nature* 460:1035–1039. <https://doi.org/10.1038/nature08229>
  41. Krammer PH (2000) CD95's deadly mission in the immune system. *Nature* 407(6805):789–795
  42. Yin X, Wang K, Gross A et al (1999) letters to nature Bid-deficient mice are resistant to Fas-induced hepatocellular apoptosis. *Nature* 400:2–7
  43. Schinzel A, Kaufmann T, Borner C (2004) Bcl-2 family members: intracellular targeting, membrane-insertion, and changes in subcellular localization. *Biochim Biophys Acta - Mol Cell Res* 1644:95–105. <https://doi.org/10.1016/j.bbamcr.2003.09.006>
  44. Migliario M, Pittarella P, Fanuli M et al (2014) Laser-induced osteoblast proliferation is mediated by ROS production. *Lasers Med Sci* 29:1463–1467. <https://doi.org/10.1007/s10103-014-1556-x>

45. Kushibiki T, Hirasawa T, Okawa S, Ishihara M (2013) Blue laser irradiation generates intracellular reactive oxygen species in various types of cells. *Photomed Laser Surg* 31:95–104. <https://doi.org/10.1089/pho.2012.3361>
46. Petros AM, Olejniczak ET, Fesik SW (2004) Structural biology of the Bcl-2 family of proteins. *Biochim Biophys Acta* 1644(2-3):83–94. <https://doi.org/10.1016/j.bbamcr.2003.08.012>
47. Grivicich I, Regner A, da Rocha AB (2007) Morte Celular por Apoptose. *Rev Bras Cancrol* 53:335–343. <https://doi.org/10.1590/S0102-311X2003000200031>